1997 HST Calibration Workshop
Space Telescope Science Institute, 1997
S. Casertano, et al., eds.

Determination of Geometric Distortion in STIS Images

Eliot M. Malumuth[1]
Hughes STX/LASP

Charles W. Bowers[1]
NASA/LASP

Abstract. This is a report on the characterization of the geometric distortion of the STIS CCD and the STIS FUV-MAMA detectors when used in imaging mode. We find that the amount of the distortion is fairly small over most of the field. The maximum displacement is 1.66 pixels for the CCD and 2.71 pixels for the FUV-MAMA. This data also allows us to determine the plate scale for both cameras. For the CCD the scale is $0\farcs05071 \pm 0\farcs00007\,\mathrm{pixel}^{-1}$. For the FUV-MAMA the scale is $0\farcs02447 \pm 0\farcs00001\,\mathrm{pixel}^{-1}$ in x and $0\farcs02467 \pm 0\farcs00002\,\mathrm{pixel}^{-1}$ in y.

1. Introduction

In order to combine HST images taken of the same field with different pointings or orientations the images must be free of spatial distortions caused by the optical path and/or detector irregularities. This is especially true if one wishes to take advantage of dithering the field at sub pixel spacings to increase the spatial resolution using techniques such as drizzle (Hook & Fruchter 1997). Thus, it is important to be able to predict or measure the distortions so that the images can be rectified in the combining process.

To measure the geometric distortion in the STIS CCD and FUV-MAMA cameras we followed a procedure similar to that used to measure the geometric distortion in the WFPC2 (Holtzman et al. 1995). For the CCD we observed the same field in the outer region of the globular cluster ω Cen observed by Holtzman et al. (1995). The central region of the cluster NGC6681 was observed for the FUV-MAMA.

2. Strategy

In principle the geometric distortion can be determined by observing a field of stars with known location and solving the following set of equations:

$$\begin{aligned} x_t &= C_0 + C_1x + C_2y + C_3x^2 + C_4xy + C_5y^2 + C_6x^3 + C_7yx^2 + C_8xy^2 + C_9y^3 \quad (1) \\ y_t &= D_0 + D_1x + D_2y + D_3x^2 + D_4xy + D_5y^2 + D_6x^3 + D_7yx^2 + D_8xy^2 + D_9y^3 \end{aligned}$$

where x_t and y_t are the true x and y positions of the stars, in pixel coordinates measured from the center of the image, and x and y are the observed positions of the stars also in pixels measured from the center of the image.

[1]Goddard Space Flight Center, Code 681, Greenbelt MD, 20771

In practice, we do not know the true location of stars in a dense enough field to map the geometry of the whole detector at once. However, moving the telescope by a known amount will put the same star in a different location on a second image. The true offsets are determined by the telescope slew and are accurate to $\sim 0''.02$. Subtracting equation 1 for a star on image 2 from equation 1 for the same star on image 1 we get:

$$\begin{aligned}(x_{t_1} - x_{t_2}) &= C_0 + C_1(x_1 - x_2) + C_2(y_1 - y_2) + C_3(x_1^2 - x_2^2) + C_4(x_1y_1 - x_2y_2) + C_5(y_1^2 - y_2^2) \\ &\quad + C_6(x_1^3 - x_2^3) + C_7(y_1x_1^2 - y_2x_2^2) + C_8(x_1y_1^2 - x_2y_2^2) + C_9(y_1^3 - y_2^3) \qquad (2) \\ (y_{t_1} - y_{t_2}) &= D_0 + D_1(x_1 - x_2) + D_2(y_1 - y_2) + D_3(x_1^2 - x_2^2) + D_4(x_1y_1 - x_2y_2) + D_5(y_1^2 - y_2^2) \\ &\quad + D_6(x_1^3 - x_2^3) + D_7(y_1x_1^2 - y_2x_2^2) + D_8(x_1y_1^2 - x_2y_2^2) + D_9(y_1^3 - y_2^3)\end{aligned}$$

where (x_1, y_1) and (x_2, y_2) are the x and y location of the star on images 1 and 2, and the quantities $(x_{t_1} - x_{t_2})$ and $(y_{t_1} - y_{t_2})$ are the known offsets between images 1 and 2 in units of pixels.

The CCD field has a large number of bright stars which fairly uniformly cover the whole field but which are not very crowded. The field was observed in a 5×5 pattern with a step size of $15''$ (~ 296 STIS CCD pixels). Figure 1 shows the center image of the pattern.

The FUV-MAMA field has a large number (over 40) of stars which are bright in the far UV and are spread out fairly uniformly over the whole $25'' \times 25''$ field of the FUV-MAMA. The field was observed in a 5×5 "plus" pattern (i.e., 9 images) with a step size of $5''$ (~ 204 STIS low-res MAMA pixels). Figure 2 shows the center image of the pattern.

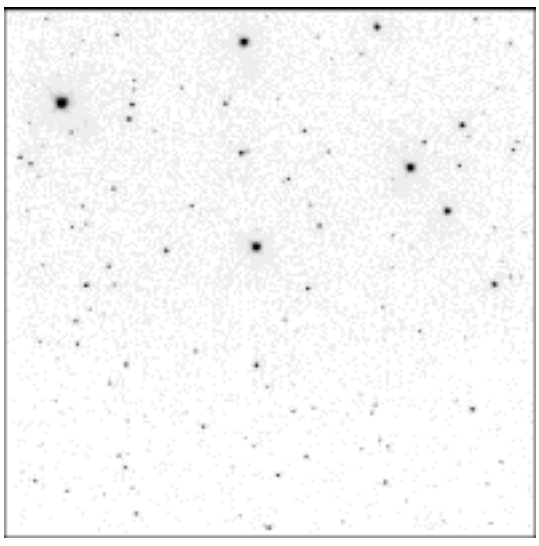

Figure 1. STIS CCD image of ω Cen (outer region). This image was the image in the center of the 5×5 pattern.

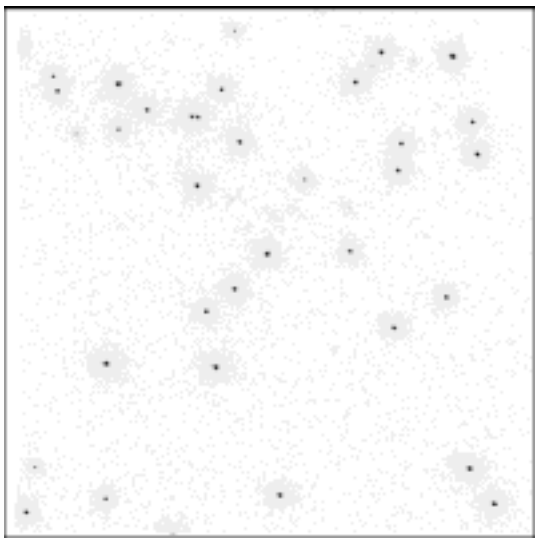

Figure 2. STIS FUV-MAMA image of NGC 6681. This image was the image in the center of the 5×5 "plus" pattern.

The special parameter POS TARG was used to move the telescope purely in the x direction, then purely in the y direction. In practice the STIS to FGS alignment isn't exactly known, therefore there was a small movement in the other coordinate as well.

3. Reductions

Each image was run through the IDL program CALSTIS to perform the standard image reduction steps and to put the data into units of counts second^{-1}. The luminosity-weighted centroid (x, y) of each star on the first image of each data set was determined using an IDL program. Next, the location and centroid of each star found on image 1 was found on the second image by using the image 1 centroids and the known offsets in x and y. Then the first program was used to find and centroid all of the stars on image 2 which were not located on image 1. This procedure was continued until each star on each image was found and its luminosity weighted centroid measured. Finally, a program which cross compared all of the star lists was run. The search was done in such a way that only succeeding images were examined so that each pair was identified only once. The resulting table listed the (x_1, y_1) and (x_2, y_2) positions of each pair (note that a star on one image could be paired with the same star on several other images—for example, CCD star #2 is on 11 images, so there are 55 pairs). In this way we found 11,338 pairs of stars for the CCD data and 834 pairs of stars for the FUV-MAMA data.

The most critical step was to determine the "true" offset between each image. We decided to use the measured star positions to determine the offsets, because the STIS to FGS alignment isn't exactly known and the pixel size isn't exactly known. The shifts between more distant images were found by summing the shifts of the images in between. No measurement of more than one step was used since the overlap region becomes small and far from the center. This procedure showed that there were some unexpected systematic effects. The telescope slews were intended to be purely in one direction or the other, however, as Figure 3 illustrates, there were small shifts in the other direction as well. Figure 3 shows the y offset of stars in the first CCD image from those in the second image (plus signs), the third image (filled circles) and the fourth image (diamonds) plotted as a function of the y position of the star. The offset is not only non-zero but a function of the y position: the higher up the chip the the larger the shift in y.

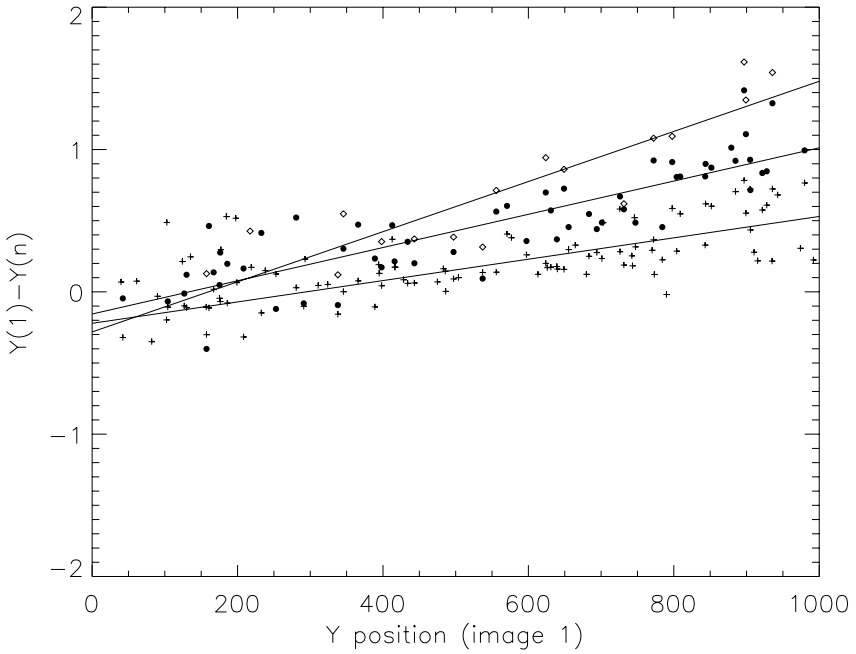

Figure 3. The difference in the y position of the same stars are shown for CCD image 1−image 2 (plus sign), image 1−image 3 (dots), and image 1−image 4 (diamonds), as a function of the y position. Notice that there is a systematic shift in the y position as a function of y.

Once the average shifts are determined, they can be subtracted from the $x_1 - x_2$ and $y_1 - y_2$ pairs to give us a measure of the extent of the distortion. If there were no distortions, all of the differences would be zero. Figure 4 shows histograms of the x and y residuals for the CCD, while Figure 5 shows the histograms for the FUV-MAMA. The RMS deviation in x was 0.410 pixels and in y was 0.375 pixels for the CCD. For the FUV-MAMA the RMS deviation in x was 0.591 pixels and in y was 0.377 pixels.

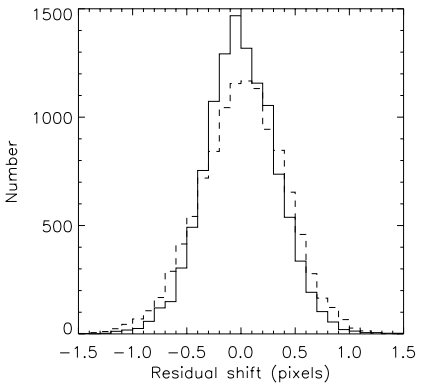

Figure 4. Histogram of the x (solid line) and y (dashed line) residuals after the average shift was subtracted from each pair for the CCD.

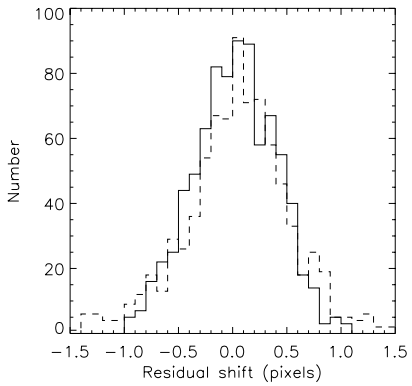

Figure 5. Histogram of the x (solid line) and y (dashed line) residuals after the average shift was subtracted from each pair for the FUV-MAMA.

An added benefit of this approach is that we can determine the scale of a pixel at the center of the image from the slews in arcseconds. For the CCD the scale is $0\farcs05071 \pm 0\farcs00007\,\mathrm{pixel}^{-1}$, with no significant difference between x and y directions. For the FUV-MAMA the scale is $0\farcs02447 \pm 0\farcs00001\,\mathrm{pixel}^{-1}$ in the x direction and $0\farcs02467 \pm 0\farcs00002\,\mathrm{pixel}^{-1}$ in the y direction. This difference between the x and y scales is due to, and consistent with, the 7.6° tilt between the FUV-MAMA camera focal plane and the detector.

A least squares matrix inversion program was used to solve the N equations (represented in Equation 2) for the 10 coefficients C_i and the 10 coefficients D_i. Note that the solution was based on a coordinate system where the central pixel was defined as $x = 0$ and $y = 0$. Thus, x = measured $x - 512.0$ and y = measured $y - 512.0$. The constant terms C_0 and D_0 are defined so that the central pixel will be $(0, 0)$ in both the corrected and uncorrected images. Table 1 shows the determined coefficients for the CCD and the FUV-MAMA images respectively.

Table 1. Geometric Distortion Coefficients

	CCD		FUV-MAMA	
i	C_i	D_i	C_i	D_i
0	0.0000000	0.0000000	0.0000000	0.0000000
1	1.0011324	-5.6351965×10^{-05}	0.9990498	-0.0001417
2	-1.2427886×10^{-04}	1.0006398	-0.0005722	1.0005972
3	-3.9052366×10^{-07}	1.4414957×10^{-07}	2.1279013×10^{-07}	6.5272699×10^{-07}
4	-2.3388352×10^{-07}	2.1911561×10^{-06}	6.1468474×10^{-06}	4.7377267×10^{-07}
5	-2.7747067×10^{-06}	-1.5699432×10^{-07}	2.3167273×10^{-06}	-2.6421370×10^{-06}
6	-5.8339901×10^{-09}	2.2058683×10^{-10}	4.6704462×10^{-09}	5.5607193×10^{-10}
7	1.4677396×10^{-09}	-3.0218644×10^{-09}	1.2221236×10^{-09}	-8.2054558×10^{-10}
8	-3.4363894×10^{-09}	8.2253175×10^{-10}	-4.5285643×10^{-09}	7.4727479×10^{-10}
9	6.8542388×10^{-10}	-3.1486902×10^{-09}	1.5149124×10^{-09}	-1.5672843×10^{-09}

The histograms of the residual differences between positions corrected using equation 1 are displayed in figures 6 and 7. The RMS residuals have been reduced to about one quarter of a pixel (CCD: $x = 0.245$ pixels, $y = 0.267$ pixels, FUV-MAMA: $x = 0.228$ pixels, $y = 0.264$ pixels).

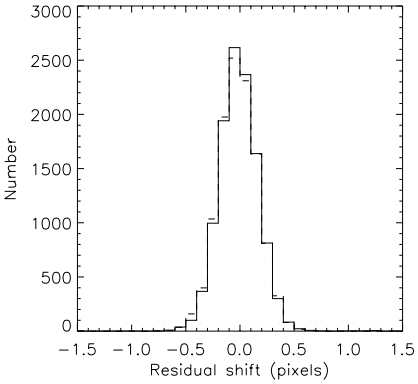

Figure 6. The same as Figure 4 except after a correction to the location of each star using Equation 1 and Table 1 was applied.

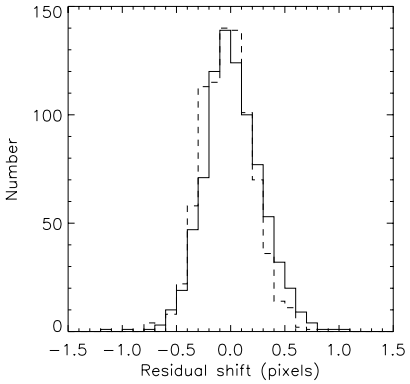

Figure 7. The same as Figure 5 except after a correction to the location of each star using Equation 1 and Table 1 was applied.

Finally, it is instructive to examine exaggerated maps of the distortion. Figures 8 (CCD) and 9 (FUV-MAMA) show the distortion pattern magnified by a factor of 50. The diamonds mark the positions where each star would be if there were no geometric distortion. The lines show the direction to where they were actually detected, the length of the line is 50 times as long as the actual displacement. The largest displacement is just over one and a half pixels (1.66 pixels) in the CCD image, while it is a little over two and a half pixels in the FUV-MAMA (2.71 pixels).

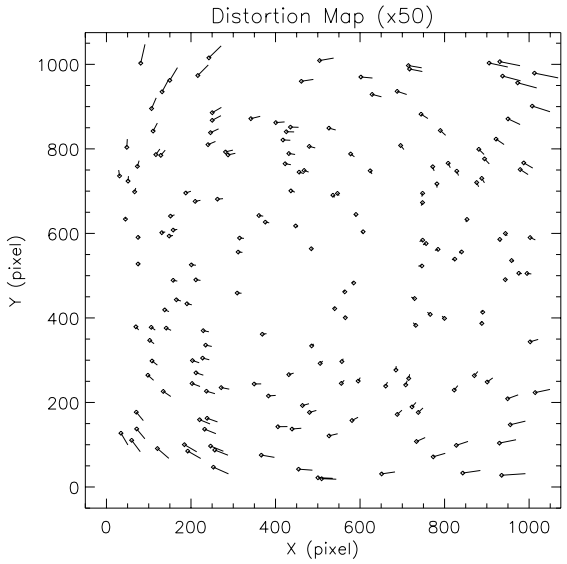

Figure 8. Map of the CCD geometric distortion magnified by a factor of 50.

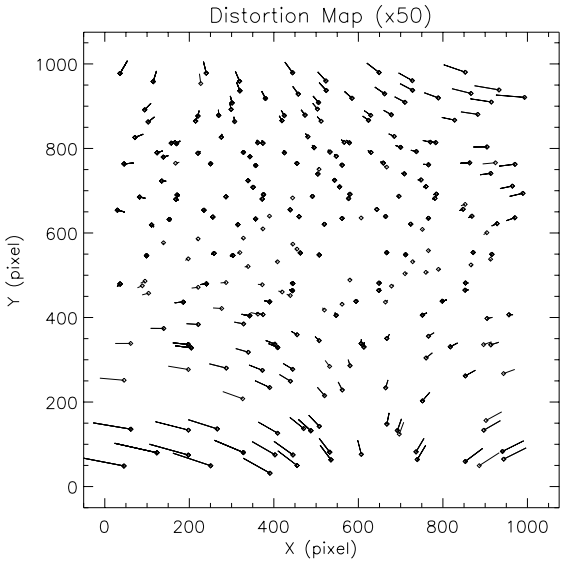

Figure 9. Map of the FUV-MAMA geometric distortion magnified by a factor of 50.

4. Applying the solution

To apply the solution we need to solve for the value of x given the true value x_t. However, what we have is the equation that gives x_t as a function of x (equation 1). The IDL program CALSTIS_UNRECTIFY written by Lindler (1997) was used to invert X and Y maps made from Equation 1 and Table 1. First, X and Y maps are made where the value in each (x, y) pixel in the X map is the value of x_t for that pixel, and the value in each (x, y) pixel in the Y map is the value of y_t for that pixel. CALSTIS_UNRECTIFY is then used to interpolate within the X and Y maps to get the $X_{\rm U}$, $Y_{\rm U}$ maps where each pixel is the value of x and y that go to the pixel value of x_t and y_t. These maps can be used to interpolate in a STIS image and produce a geometrically corrected image.

An alternative method of applying the solution is to invert the equation and determine the value of the measured position as a function of the true positions. All of the measured positions of all of the stars on all of the images and coefficients C and D from above were used to determine the true positions (x_t,y_t) for all of the stars. We then used Equation 1 (with x_t substituted for x and y_t substituted for y, etc.) to solve for the coefficients C_t and D_t which will give the value of x and y as functions of x_t and y_t. These coefficients are given in Table 2.

Table 2. Correction Coefficients

	CCD		FUV-MAMA	
i	C_{t_i}	D_{t_i}	C_{t_i}	D_{t_i}
0	0.0000000	0.0000000	0.0000000	0.0000000
1	0.9988664	5.6727465×10^{-05}	1.0009502	0.0001418
2	0.0001248	0.9993592	0.0005731	0.9994030
3	3.9591137×10^{-07}	-1.4366138×10^{-07}	-2.0869856×10^{-07}	-6.5273543×10^{-07}
4	2.3331625×10^{-07}	-2.1919157×10^{-06}	-6.1460401×10^{-06}	-4.7437861×10^{-07}
5	2.7776938×10^{-06}	1.5749193×10^{-07}	-2.3189523×10^{-06}	2.6408455×10^{-06}
6	5.8428546×10^{-09}	-2.2236194×10^{-10}	-4.6635149×10^{-09}	-5.5504118×10^{-10}
7	-1.4750553×10^{-09}	3.0328006×10^{-09}	-1.2247637×10^{-09}	8.2536032×10^{-10}
8	3.4351917×10^{-09}	-8.2897208×10^{-10}	4.5476076×10^{-09}	-7.4670016×10^{-10}
9	-6.8621846×10^{-10}	3.1482116×10^{-09}	-1.5125294×10^{-09}	1.5814600×10^{-09}

References

Holtzman, J., et al., 1995, PASP, 107, 156

Hook, R. N. & Fruchter, A. S., 1997, in *Astronomical Data Analysis Software and Systems VI*, A.S.P. Conf. Ser., Vol. 125, eds. G. Hunt and H. E. Payne (San Francisco: ASP), 147

Lindler, D., 1997, private communication